링의 변형율 이용한 저항용접 전류측정장치의 개발

New Current Measurement Device in Resistance Spot Welding by Using the Ring Deformation

S.–W. Park*, and S.–J. Na**

* Now in Agency for Defense Development

** Korea Advanced Institute of Science and Technology Dept. of Production Eng.

OVERVIEW

A new method was investigated to measure the high current in resistance welding processes. A measuring unit was developed by using a strain gage attached on the outer surface of a steel ring. The steel ring was placed around a section of the secondary loop of the welding machine, and was deformed by electro–magnetic forces induced by the high welding current. The circumferential constituent of the ring deformation was then used to obtain a signal voltage proportional to the secondary welding current. The strain gage signal of ring deformation is enough to determine the welding current in resistance spot welding, especially when welded with direct current.

FUNDAMENTAL THEORY

Gapless Solid Ring

Consider the magnetic circuit of a closed ring of uniform cross section A and mean length l, Fig.1. Suppose that the welding current I is flowing in the secondary circuit of the welding machine, and that the secondary circuit passes through the steel ring. The flux density B in the steel ring can be then expressed as follows [1].

$$B = \mu \cdot H_r = \frac{\mu \cdot I}{l} = \frac{\mu \cdot I}{2\pi R} \qquad (1)$$

where μ is the permeability of the ring material (in this study, its permeability assumed to be uniform) and H_r is the magnitude of magnetic field in the ring. The density of energy stored in the magnetic field of ring can be expressed in the following equation.

$$w_m = \frac{1}{2} \cdot \frac{B^2}{\mu} \qquad (2)$$

The total energy stored in the ring is

$$W_m = w_m \cdot A \cdot l = \frac{\pi \cdot A \cdot R \cdot B^2}{\mu} = \frac{A^2 \cdot \mu \cdot I^2}{2\,(2\pi R \cdot A)} = \frac{A^2 \cdot \mu \cdot I^2}{2\,V} \qquad (3)$$

where $V = 2\pi R \cdot A$ is the volume of the ring. If the cross–sectional area A of the ring is assumed to be remain constant during deformation, the following formula can be obtained.

$$dW_m = \frac{\partial W_m}{\partial V} \cdot dV = -\frac{A^2 \cdot \mu \cdot I^2}{2\,V^2} \cdot dV \qquad (4)$$

But energy may also be expressed as stress times volume change, which in this case is $-P \cdot dV$, where P is the circumferential compressive stress in the ring. Thus

$$P = \frac{A^2 \cdot \mu \cdot I^2}{2\ V^2} = \frac{\mu \cdot I^2}{8\ \pi^2 \cdot R^2} \qquad (5)$$

If the ring deformation remains within its proportional limits, the circumferential strain, which will be measured by using a strain gage, can be expressed as follows,

$$\epsilon_\theta \cong \frac{P}{E} = \frac{\mu \cdot I^2}{8\ \pi^2 \cdot E \cdot R^2} \qquad (6)$$

where E is the Young's modulus of ring material. ϵ_θ can be considered as proportional to I^2 in resistance spot welding, where extremely high magnetic fields are caused by the high secondary currents, and at high values of H the permeability can be assumed to be constant[2].

Ring with an Air Gap

Let a narrow air gap of thickness g be cut in the steel ring, as shown in Fig. 2(a). The gap detail is presented in Fig. 2(b). Because of the continuity of the normal component of B the flux density in the gap is the same as in the steel if fringing is neglected.

$$B = \mu \cdot H_r = \mu_o \cdot H_g \qquad (7)$$

where μ_o is the permeability of air and H_g is the magnitude of the magnetic field in the air gap. Applying Ampere's law, the following relationship can be obtained.

$$\oint \mathrm{H} \cdot \mathrm{dl} = H_r \cdot (l - g) + H_g \cdot g = I \qquad (8)$$

Substituting (7) into (8), B can be described by the following formula.

$$B = \frac{I}{(\frac{l-g}{\mu} + \frac{g}{\mu_o})} = \frac{I}{(\frac{2\pi R - g}{\mu} + \frac{g}{\mu_o})} \qquad (9)$$

The total energy stored in air gap and ring can be determined by considering the energy density in two media $\frac{1}{2}\frac{B^2}{\mu_o}$ and $\frac{1}{2}\frac{B^2}{\mu}$ respectively. Thus

$$W_m = \frac{1}{2}\frac{B^2}{\mu_o} \cdot A \cdot g + \frac{1}{2}\frac{B^2}{\mu} \cdot A \cdot (2\pi R - g) = \frac{1}{2} A \cdot \frac{I^2}{(\frac{L}{\mu} + \frac{g}{\mu_o})} \qquad (10)$$

where $L = 2\pi R - g$ is the length of ring. Supposing that the length of the ring L is maintained constant during changes in g, the energy stored in the air gap and the ring is increased by the infinitesimal amount

$$dW_m = \frac{\partial W_m}{\partial g} \cdot dg = -\frac{1}{2} A \cdot I^2 \cdot \frac{\frac{1}{\mu_o}}{(\frac{L}{\mu} + \frac{g}{\mu_o})^2} \cdot dg \qquad (11)$$

But energy may also be expressed as force times distance, which in this case is $-F \cdot dg$,

where F is the attractive force between the poles. Thus

$$F = \frac{1}{2} A \cdot I^2 \cdot \frac{\frac{1}{\mu_0}}{\left(\frac{L}{\mu} + \frac{g}{\mu_0}\right)^2} = \frac{1}{2} A \cdot \frac{\mu_0 \cdot \mu^2}{\left\{\mu_0 \cdot (2\pi R - g) + \mu \cdot g\right\}^2} \cdot I^2 \qquad (12)$$

Dividing F by A, the stress P_t at the ends of the ring can be expressed as follows

$$P_t = \frac{\mu_0 \cdot \mu^2}{2\left\{\mu_0 \cdot (2\pi R - g) + \mu \cdot g\right\}^2} \cdot I^2 = \frac{\mu \cdot I^2}{8\pi^2 \cdot R^2} \cdot \frac{1}{K} = \frac{P}{K} \qquad (13)$$

where $K = \left(\frac{1}{4\pi^2} \cdot \frac{\mu}{\mu_0} - \frac{1}{2\pi^2} + \frac{1}{4\pi^2} \cdot \frac{\mu_0}{\mu}\right) \cdot \left(\frac{g}{R}\right)^2 + \left(\frac{1}{\pi} - \frac{1}{\pi} \cdot \frac{\mu_0}{\mu}\right) \cdot \left(\frac{g}{R}\right) + \frac{\mu_0}{\mu}$

Assuming that the ratio of permeability $\frac{\mu}{\mu_0}$ is 3000 [2], the K–value becomes 1(unit) for $\frac{g}{R}$ = 0.1149, and increases with increasing $\frac{g}{R}$. That is, P_t is greater than P(the compressive stress in the solid ring), if $\frac{g}{R}$ can be maintained smaller than 0.1149.

Let a strain gage be attached on the outer surface of the steel ring, opposite to the air gap, Fig. 3. If the bending moment and compressive stress are simply considered, the circumferential strain sensed by the strain gage can be expressed as follows,

$$\epsilon_\theta = \frac{2\,R \cdot F \cdot c}{E \cdot I_m} - \frac{F}{E \cdot A} = \frac{\mu \cdot I^2}{8\pi^2 \cdot R^2} \cdot \frac{1}{K \cdot E} \cdot \left(\frac{2\,R \cdot c}{I_m} - \frac{1}{A}\right) \qquad (14)$$

where I_m is the second moment of the ring cross–sectional area and c is the distance of the strain gage from the neutral plane.

EXPERIMENTS AND DISCUSSION

Three types of experimental ring were fabricated using a steel pipe of low carbon content. The first type of ring was a closed ring of uniform cross section, as shown in Fig. 1, while the second type was a ring with a small air gap, as shown in Fig. 2. The third type of ring is illustrated in Fig. 4. In this type, a closed ring was used to increase the rigidity of the measuring device, when compared to the ring with an air gap. However a part of the ring was machined to have a U–groove, which establishes a curved cantilever from the closed ring. A strain gage was then attached at a place near the places of attachment of the cantilever. This is where the bending moment has its maximum value under an external load at the free end of the cantilever. The pipe material was fully annealed before machining to minimize the possible initial distortion which may occur through the release of residual stresses in the steel pipes.

A series of experiments was carried out on a three–phase direct current spot welding machine, the nominal input at 50 % duty cycle of which is 96 kVA (3 x 32 kVA). The short–circuit current of the machine is 60 kA. The welding current was varied by a digital controller, which determines the firing phase of the thyristor by means of percent (%). Three different welding currents (20, 40 and 60 %) were applied to test the experimental rings. The gain of the amplifiers was chosen to be the same in all experiments to compare the sensitivity and response characteristics of the current measurement devices. The welding process was composed of three stages, that is, current up–slope, main current and

current down–slope stage. The duration of current up–slope and down–slope stage was fixed at 3 cycles, while the duration of main current stage on 10 cycles.

Some typical measured results of the closed ring unit are shown in Fig. 5. The 20 % welding current results in a lower strain gage output signal than the 40 or 60 % current, as can be expected from the theory. However the 40 and 60 % currents show almost the same magnitude of strain gage signal. It can also be stated that the response of the strain gage is very unstable at the beginning and end of the welding process. This is especially true at the beginning, when the ring begins to deform. These instabilities are believed to be due to the initially incomplete ring shape and to the nonuniform deformation of the ring during the current flow. A small impact on the ring would have caused a considerable difference in measured results.

Figure 6 shows typical measured strain gage signals for the ring with the small air gap. Three different welding currents result in almost the same variation trend of strain gage signal. At the beginning of the welding process, it increases very rapidly, then it reaches its maximum and decreases to a lower magnitude. Near the end of the process it again increases to a maximum and then decreases very rapidly. The second maximum is almost the same as the first maximum. The rapid increase and decrease are probably due to the bending of the ring with the air gap, which occurs at the moment of current flow. But very soon after the welding start, the ends of air gap are brought into contact. Then the ring begins to work like a closed ring, in which the electromagnetic force causes a compressive stress. This compressive stress component then reduces the tensile stress component of the bending moment and consequently the strain gage signal. The signal fluctuation which occurred after the end of current flow is believed to be caused by the inadequate rigidity of the device.

Figure 7 shows the typical measured results of the cantilever–type ring device. Three different welding currents generate the evidently distinguishable strain gage signals, which increase with increasing current. This strain gage signal is stable throughout in the whole welding process, and that the up–slope and down–slope stages are also more or less proportional to the welding current.

Figure 8 (a) represents the result of the cantilever device's strain profile during welding process for complex current setting. For comparison of the result of the new method with other conventional method, the troidal coil was used for measuring the welding current. The output signal of the troidal coil was acquired by the data acquisition system, and integrated. These integrated troidal signals were also show in Fig. 8 (b). These figures reveal that the results of the cantilever device and that of the conventional method were nearly identical though some small discrepancy was found. Hence, the current profiles during welding process may be easily measured by using the new device.

REFERENCES

[1] J.D.Kraus and K.R.Carver, *Electromagnetics.* New York, NY : McGraw–Hill, 1973

[2] A.Shadowitz, *The Electromagnetic Field.* New York, NY : McGraw–Hill, 1975

[3] G.R.Archer, "A new system for automatic feedback control of resistance spot welding," *Welding J.*, pp. 987–993, Oct. 1959

[4] D.N.Waller, "Head movement as a means of resistance welding quality control," *British Welding J.*, pp. 118–122, Mar. 1964

[5] S.Bhattachava and D.R.Andrews, "Resistance–weld quality monitoring," *Sheet Metal Industries*, pp. 460–466, July 1972

[6] O.E.Martin, "Resistance weld for maintaining weld quality," *Welding J.*, pp. 655–660, Aug. 1976

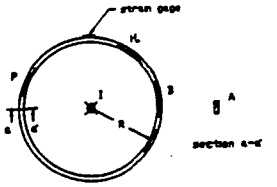

Fig. 1 Closed steel ring with secondary welding circuit

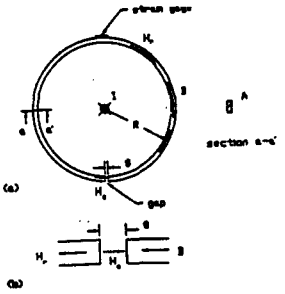

Fig. 2 Steel ring with air gap

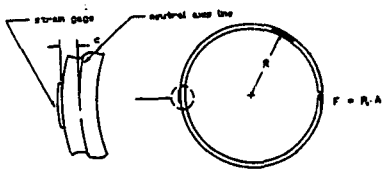

Fig. 3 Strain gage on steel ring with air gap

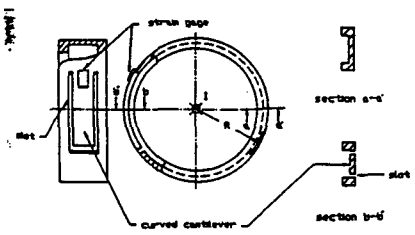

Fig. 4 Closed steel ring with curved cantilever

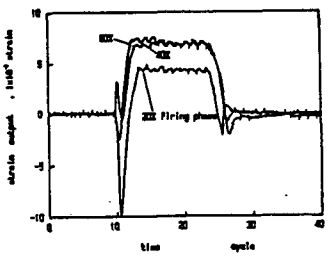

Fig. 5 Current measurement results of closed ring

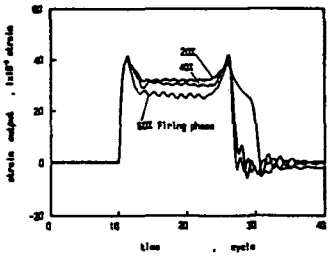

Fig. 6 Current measurement results of ring with air gap

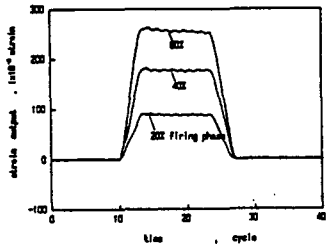

Fig. 7 Current measurement results of closed ring with cantilever part

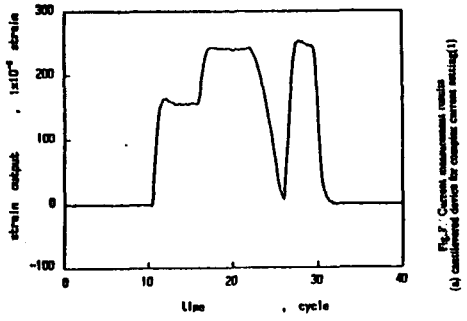

Fig. 8 Current measurement results (a) cantilevered device for complex current setting(1)

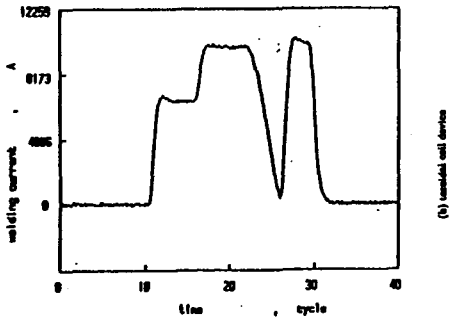

(b) toroidal coil device